

# The stretching of Hercules<sup>\*</sup>

A. J. Deason<sup>1</sup>†, V. Belokurov<sup>1</sup>, N. W. Evans<sup>1</sup>, L. L. Watkins<sup>2</sup>, M. Fellhauer<sup>3</sup>

<sup>1</sup>*Institute of Astronomy, Madingley Rd, Cambridge, CB3 0HA*

<sup>2</sup>*Max-Planck-Institut für Astronomie, Königstuhl 17, Heidelberg, 69117, Germany*

<sup>3</sup>*Departamento de Astronomia, Universidad de Concepcion, Casilla 160-C, Concepcion, Chile*

July 2012

## ABSTRACT

We present VLT/FORS2 spectroscopy of candidate blue horizontal branch (BHB) stars in the vicinity of the Hercules ultrafaint dwarf galaxy. We identify eight convincing Hercules BHB members, and a further five stars with similar systemic velocities to that of Hercules, but  $\sim 0.5$  kpc from the centre of the galaxy along its major axis. It is likely that these stars once belonged to Hercules, but have been tidally stripped and are now unbound. We emphasise the usefulness of looking for any gradient in the systemic velocity of this stretched system, which would further support our interpretation of the origin of its elongated and distended morphology.

**Key words:** galaxies: dwarf – galaxies: interactions – galaxies: kinematics and dynamics, Local Group

## 1 INTRODUCTION

What made the Ultra Faint dwarf (UFD) satellites so fluffy? Their low present-day stellar densities could either be the consequence of stunted star-formation, or possibly result from sustained pummelling by Galactic tides. These two hypotheses are not mutually exclusive: an intrinsically faint galaxy can be further thinned down. Periodic tidal encounters in the host potential (especially in the presence of a disc) are known to lead to a gradual decrease in all structural parameters of the satellite: its stellar density, size and velocity dispersion will all be diminished (Peñarrubia et al. 2010). As the torn stars start to arrange themselves along the satellite’s orbit, the stellar density contours become more elongated, until the bound object dissolves into a tidal stream. In the Milky Way, the best example of a satellite galaxy in the process of tidal disruption is the Sagittarius dwarf with the apparent remnant ellipticity of 0.65 (e.g. Majewski et al. 2003). In several UFDs, suspiciously high ellipticities have been measured, with UMa I (Martin et al. 2008), UMa II (Zucker et al. 2006; Muñoz et al. 2010) and Hercules (Belokurov et al. 2007) all having  $\epsilon \geq 0.5$ . Additional observations are needed to tell whether the high ellipticity of stellar density contours in these objects is a symptom of tidal influence or an intrinsic property of the satellite, and hence the signature of the processes at the epoch of formation<sup>1</sup>.

Of the several “elongated” Galactic satellites, Hercules is one

that clearly stands out based on mounting evidence that its density profile extends further than indicated by the nominal half-light radius ( $r_h \sim 0.3$  kpc, Belokurov et al. 2007). Deep follow-up imaging of Hercules by Coleman et al. (2007) and Sand et al. (2009) helped to confirm its elongation and led to the identification of possible tidal arm features beyond twice the half-light radius. While these extensions are identified in the number counts of candidate red giant branch (RGB) stars, there is also an over-density of possible blue horizontal branch (BHB) stars coincident with the detections. These BHB candidates offer the prospect of a straightforward and independent confirmation of the narrow stellar tail: at such blue colours, the Galactic foreground contamination is minimal, even at faint ( $r > 21$ ) magnitudes corresponding to Hercules’ distance.

Early spectroscopic work on Hercules was confined to the central half-light radius (Simon & Geha 2007). More recently, Adén et al. (2009b) concluded that, compared to the original study of Simon & Geha (2007), their data (presented in Adén et al. 2009a) indicated a lower total mass for this system based on the smaller velocity dispersion measurement, reduced primarily due to efficient interloper identification. Intriguingly, they also draw attention to a possible velocity gradient along the major axis of the system which might be indicative of tidal stretching. To clarify the nature of the stellar extension to Hercules, we have used FORS2 on the Very Large Telescope (VLT) to obtain spectra of some of the BHB candidates superposed onto the RGB over-density, both in the central region of the galaxy, and its very outskirts. In this Letter, we present the results of this follow-up campaign and compare our findings to those of the previous spectroscopic studies.

<sup>\*</sup> Based on observations made with ESO Telescopes at the La Silla Paranal Observatory under programme ID 083.B-0269(A)

† E-mail: ajd75, vasily.nwe@ast.cam.ac.uk

<sup>1</sup> However, it is also worth bearing in mind that Poisson noise can often account for the appearance of elongated shapes in low density maps of ultrafaint systems (see e.g. Martin et al. 2008; Muñoz et al. 2012)

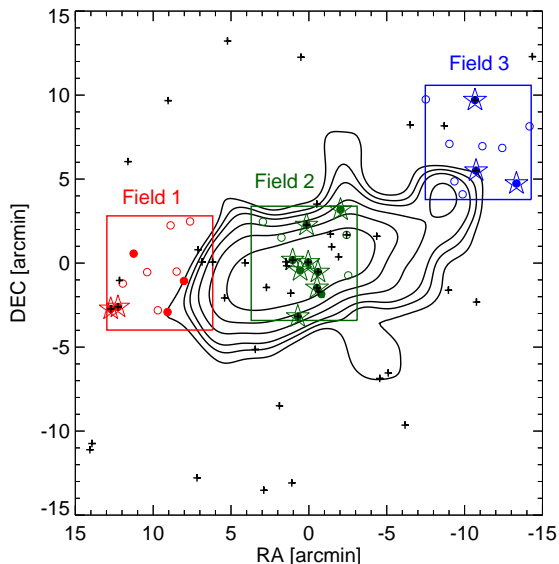


**Figure 1.** The distribution of candidate BHB stars are over-plotted on the density distribution of RGB stars for the Hercules ultra-faint dwarf spheroidal. The black contours are derived from the imaging presented in Sand et al. (2009) and show the density contrast of stars in the vicinity of the Hercules dwarf relative to the field. The density of stars is smoothed with a 1 arcminute Gaussian and the contours show the 3, 4, 5, 7, 10 and 15  $\sigma$  levels. The open circles are candidate Hercules member stars (inc. BHB and RGB stars) targeted in this study and filled circles show stars with useful spectra. The plus signs mark all potential BHB targets. The star symbols indicate stars which are likely Hercules dSph members (see Section 3). The stars are coloured according to the field they belong to (this colour scheme is adopted throughout this study). The boxes show the FORS2 MOS fields-of-view.

## 2 OBSERVATIONS

### 2.1 Target Selection

Candidate BHB stars were selected from Sloan Digital Sky Survey data release 7 photometry on the basis of their colours and vicinity to the Hercules dwarf spheroidal galaxy. Specifically, we applied the following cuts in absolute magnitude and  $u - g, g - r$  colours (cf. Sirko et al. 2004):

$$\begin{aligned} 0.5 < u - g < 1.7 \\ -0.6 < g - r < 0.15 \\ -0.5 < M_g < 2 \end{aligned} \quad (1)$$

Here, the absolute magnitude is estimated from the apparent  $g$  band magnitude assuming a distance modulus of 20.625 for Hercules (Sand et al. 2009). The distribution of these candidate stars is shown in Fig. 1. We target three fields along the major axis of Hercules; the outer fields are approximately 0.5 kpc from the centre and are chosen to probe the apparent extended structure of the dwarf galaxy.

### 2.2 VLT-FORS2 spectroscopy

Follow-up spectroscopic observations were made with the VLT-FORS2 instrument in multi-object spectroscopy (MOS) mode. In this mode, there are 19 movable slits in a  $6.8 \times 6.8$  arcmin<sup>2</sup> field-of-view. This setup nicely matches the number of candidates we ex-

Field No.	RA (J2000)	DEC (J2000)	# targets extracted	# useful spectra	# members
1	16:31:40.22	+12:46:55.91	11	5	2
2	16:31:03.14	+12:47:30.31	13	9	8
3	16:30:17.41	+12:54:42.12	10	3	3

**Table 1.** VLT-FORS2 Masks: We give the Field number, the central right ascension and declination, the number of objects targeted, the number of useful spectra and the number of likely Hercules members.

pect to obtain with each field of view. We use the GRIS1400V+18 grism, with a wavelength range of  $\lambda \sim 4560 - 5860$  Å to target the strong  $H\beta$  line at  $\lambda 4861$  Å. Observations were taken in 2009 April-May with typical exposure times of 1.5h per field with 0.8 arcsecond slits in conditions well-matched to the slit width.

The spectroscopic data were reduced using the standard esorex pipeline provided by ESO. The science frames are bias subtracted and flat-fielded and the sources are extracted after aligning the slits. The wavelength calibration was applied with reference to a HeNe/MgCd lamp. Calibration frames are typically taken in the daytime and there can be significant changes in daytime to nighttime conditions (e.g. slight changes in the slit positions). Thus, comparing the wavelength calibration to strong sky lines (e.g. OI  $\lambda 5577$  Å) is required to make fine corrections to the wavelength solution. However, in some cases the spectral range did not include such strong skylines and significant velocity differences were seen between observations of the same star taken at different times. These few (3 objects, all in Field 2) cases are excluded from our sample as shifts of  $\sim 1$  Å are possible. (or  $V_{\text{rad}} \sim 60$  km s<sup>-1</sup> at  $\lambda \sim 4861$  Å).

The uncertainty in the wavelength calibration and skyline shifts leads to a systematic error in the velocity of approximately 6 km s<sup>-1</sup>, which we later add in quadrature to the measured velocity uncertainties. With this relatively low resolution spectrograph ( $R \sim 2000$ ), and one strong Balmer line we cannot get accurate enough velocities to measure the velocity dispersion or velocity gradients in the dwarf galaxy, but we can confirm membership. Follow-up, higher-resolution spectroscopy with a larger wavelength coverage (ideally covering several strong Balmer lines), is required to investigate these points further.

Table 1 summarises the observations for each field. Spectra are defined as ‘useful’ if we can measure a velocity from the  $H\beta$  line. Typical un-useful cases include QSOs, noisy spectra, no  $\lambda 5577$  Å skyline and/or no  $H\beta$  coverage. Note that our main aim is to target BHB stars, but we may also have red horizontal branch-asymptotic giant branch (RHB-AGB) or red giant branch (RGB) stars in the field of view. To measure the radial velocities, we fit Sersic profiles to the  $H\beta$  line using the IDL MPFIT<sup>2</sup> program (Markwardt 2009). The flux is normalised by fitting the continuum away from the line centre. The model profiles are convolved with the full-width-half-maximum (FWHM) resolution ( $\sim 4$  Å).

## 3 RESULTS

The list of candidate Hercules dSph galaxy members are given in Table 2. The radial velocities of these stars are shown in Fig. 2 in order of right ascension. Encouragingly, our candidate members

<sup>2</sup> MPFIT is available from <http://purl.com/net/mpfit>

ID	RA [deg]	DEC [deg]	R [pc]	$g - i$	$r$	Type	$V_{\text{rad}}$ [km s $^{-1}$ ]	$V_{\text{herc}}$ [km s $^{-1}$ ]	$N_{\text{Besoc}}$	Class	Aden09 ID
F1-09	247.9701	12.7466	520.9	-0.31	21.28	BHB	$7 \pm 11$	$-38 \pm 11$	0.0	H	—
F1-10	247.9624	12.7485	501.8	-0.35	21.26	BHB	$33 \pm 11$	$-12 \pm 11$	0.1	H	—
F1-21	247.9456	12.8014	450.6	0.61	21.32	RGB	$-10 \pm 19$	$55 \pm 19$	1.5	H/F	—
F1-16	247.9093	12.7434	382.0	0.81	20.02	RHB-AGB	$47 \pm 7$	$2 \pm 7$	3.0	H/F	40435
F1-19	247.8917	12.7743	323.5	0.93	21.21	RGB	$25 \pm 35$	$20 \pm 35$	1.7	H/F	—
F2-06	247.7754	12.7951	43.0	-0.51	21.28	BHB	$61 \pm 13$	$16 \pm 13$	0.0	H	—
F2-09	247.7699	12.7390	133.0	-0.37	21.27	BHB	$40 \pm 14$	$-5 \pm 14$	0.1	H	—
F2-05	247.7674	12.7845	29.0	-0.59	22.18	BHB	$7 \pm 38$	$38 \pm 38$	0.1	H	—
F2-16	247.7605	12.8298	93.6	-0.27	21.28	BHB	$31 \pm 12$	$-14 \pm 12$	0.1	H	—
F2-07	247.7588	12.7927	3.5	0.27	21.07	Variable	$65 \pm 16$	$20 \pm 16$	0.3	H	—
F2-12	247.7493	12.7674	63.3	-0.06	20.32	Variable	$64 \pm 8$	$19 \pm 8$	0.0	H	42113
F2-17	247.7483	12.7832	31.1	-0.44	21.32	BHB	$27 \pm 12$	$-18 \pm 12$	0.0	H	42134
F2-20	247.7448	12.7613	81.4	0.85	20.55	RGB	$50 \pm 8$	$5 \pm 8$	2.6	H/F	—
F2-01	247.7242	12.8450	153.7	0.27	20.31	RHB-AGB	$65 \pm 10$	$20 \pm 10$	0.1	H	—
F3-02	247.5802	12.9537	583.0	-0.12	21.00	BHB	$32 \pm 12$	$-12 \pm 12$	0.0	H	35570
F3-03	247.5792	12.8839	484.7	0.02	21.15	BHB	$80 \pm 12$	$35 \pm 12$	0.0	H	—
F3-07	247.5359	12.8710	566.8	-0.26	21.58	BHB	$30 \pm 15$	$-15 \pm 15$	0.1	H	—

**Table 2.** Candidate Hercules dSph galaxy members. Column 1 lists the target ID. Columns 2 and 3 list the coordinates (J2000). Column 4 gives the projected distance from the centre of Hercules. Column 5 gives the  $g - i$  SDSS colour and Column 6 gives the SDSS  $r$ -band apparent magnitude. All given magnitudes/colours are extinction corrected according to Schlegel et al. (1998). Column 7 lists the evolutionary state of the star (based on photometry). Column 8 lists the (heliocentric) radial velocity and Column 9 lists the line of sight velocity relative to the systematic velocity of Hercules ( $45 \text{ km s}^{-1}$ ). Column 10 gives the number of stars predicted by the Besançon model in the colour, magnitude and velocity range (within  $1\sigma$  errors) of the candidate Hercules member. Column 11 lists the classification of the star based on the expected field contamination by the Besançon model (H=Hercules member, H/F= tentative Hercules member due to high field contamination). Column 12 gives the ID from Adén et al. (2009a) if applicable.

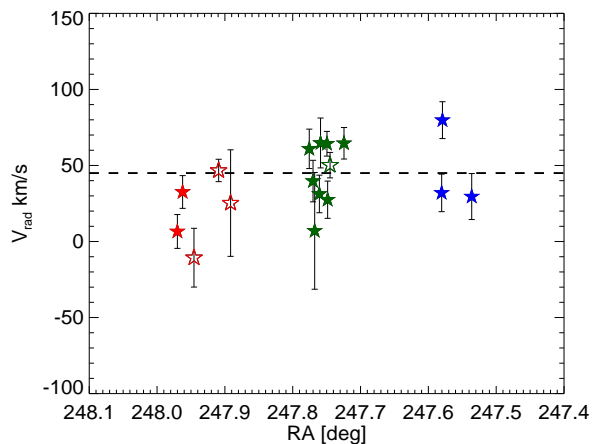


**Figure 2.** The heliocentric velocity of candidate Hercules dSph member stars against their right ascension. The solid line indicates the systemic velocity of Hercules ( $V_{\text{rad}} = 45 \text{ km s}^{-1}$ ). The filled star symbols indicate likely Hercules dSph members while the un-filled star symbols indicate likely field stars (see text for more details on this classification)

have radial velocities which cluster around the systemic velocity of Hercules ( $V_{\text{rad}} = 45 \text{ km s}^{-1}$ , Simon & Geha 2007; Adén et al. 2009a).

We quantify the level of field contamination in our sample using the Besançon Galaxy model (Robin et al. 2003). A mock sample of Milky Way stars is generated over  $10 \text{ deg}^2$  centred on the Hercules dSph co-ordinates. We consider all stellar populations in both the halo and disk components of the Galaxy. The Besançon model does not include the main contaminant of BHB stars, namely blue straggler stars (BS), which we add by hand by cloning the model BHBs and increasing their apparent magnitudes by 2 mags

(see e.g. Deason et al. 2011)<sup>3</sup>. For each candidate Hercules member in our sample, we estimate the expected number of the Galactic foreground by adding together the Besançon model counts in the star’s vicinity in the 3D space comprised of  $g - r$ ,  $r$  and  $V_{\text{rad}}$ . The contribution of each model star to the total is weighed according to the Gaussian probability that the true colour, magnitude and velocity values of the observed star lie at this location. These numbers of expected Galactic contamination are then scaled down by the ratio of  $10 \text{ deg}^2$  to the area covered by the three VLT-FORS2 fields ( $3 \times 0.1 \text{ deg}^2$ ) and are given in column 10 in Table 2. To estimate the actual posterior probability of the observed star belonging to the Hercules dSph given its 3D coordinates, one would additionally require a model for the probability density of the Hercules population. However, we note that in our sample the estimated Galactic signal is highly bimodal: for all BHB/RHB stars the Besançon model predicts insignificant contamination, while for each AGB/RGB candidate several model stars are expected. Therefore, the Hercules membership probability is likely to be close to 1 for the BHB/RHBs irrespectively of the model for the dwarf galaxy’s pdf, but is highly dependant on the details of such model for the redder AGB/RGB candidates. Therefore, we classify all BHB/RHB candidates as the most probable Hercules members and all redder stars as tentative members.

The velocity distribution of stars in the Besançon model (in the direction of Hercules) roughly follows a Gaussian distribution centred on a velocity  $V_{\text{rad}} \sim -100 \text{ km s}^{-1}$  (with a dispersion of  $\sigma \sim 100 \text{ km s}^{-1}$ ). The systemic velocity of Hercules ( $45 \text{ km s}^{-1}$ ) lies in the wing of this distribution. Thus, velocity measurements are an important discriminant between members and non-members.

The left hand panel of Fig. 3 shows a colour-magnitude diagram (CMD) for the Hercules dSph galaxy. The black circles show potential targets for this spectroscopic program and the star symbols indicate the spectroscopically confirmed members. The

<sup>3</sup> Here, we assume a 1:1 ratio between BHB and BS stars, but our results are unchanged if the BS-to-BHB ratio increases to 3:1

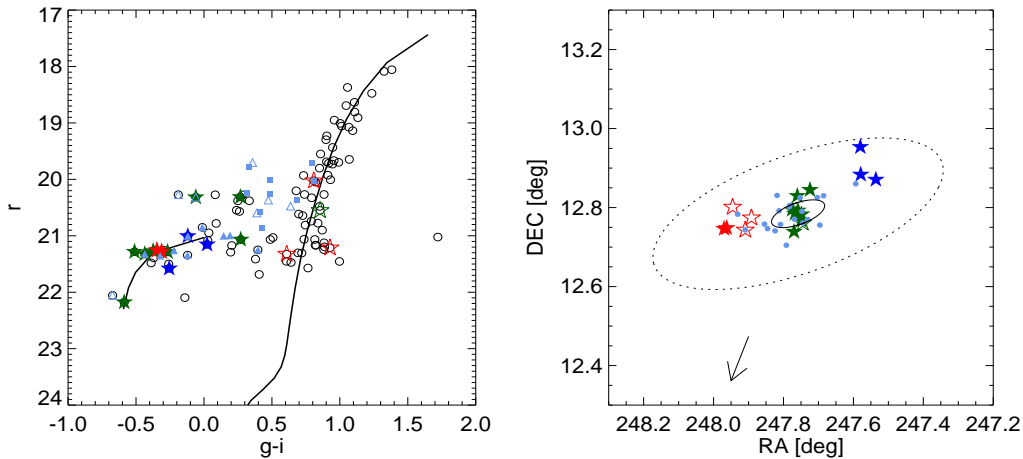


**Figure 3.** Left panel: A colour-magnitude diagram for the Hercules dSph galaxy. The open symbols indicate potential Horizontal branch ( $g - r < 0.15$ ) and RGB-AGB or RGB ( $g - r > 0.15$ ) members selected with absolute magnitudes in the distance range of Hercules. The blue filled squares, filled triangles and open triangles show photometrically selected RHB-AGB, BHB and variable star members by Adén et al. (2009a). The star symbols indicate the stars from this study which we consider likely members of the Hercules dSph. Open star symbols indicate RGB stars which are more tentative members owing to high field contamination. Fiducial stellar population sequences in the globular cluster M92 are shown by the black curves (data from Clem et al. 2008). These are corrected for Galactic extinction and shifted to a distance of  $D = 140$  kpc (Belokurov et al. 2007). Right panel: The spatial distribution of Hercules member stars. The blue points are spectroscopically confirmed RGB (+2 RHB-AGB) stars by Adén et al. (2009a). The solid and dotted ellipses indicate the core radius and the King profile limiting radius derived by Coleman et al. (2007). The arrow indicates the direction to the Galactic Centre.

blue squares and triangles show photometrically selected RHB-AGB and BHB star members by Adén et al. (2009a). In addition, the open blue triangles show the stars that Adén et al. (2009a) infer to be variable stars belonging to the Hercules dSph. Four of our confirmed members overlap with this study (see Table 2), but Adén et al. (2009a) only measured a velocity for one of these stars. The black curves show fiducial stellar population sequences for the globular cluster M92 derived from Clem et al. (2008) shifted to the distance of Hercules ( $D \sim 140$  kpc, Belokurov et al. 2007). Sand et al. (2009) showed that this old, metal poor population is a good fit to the Hercules CMD (see also Simon & Geha 2007). Our Hercules member stars fall nicely onto these fiducial evolutionary tracks. In Table 2 we give an estimate of the evolutionary stage of the stars according to their position on the CMD. Note that we classify two stars as possible variable stars belonging to the Hercules dSph. One of these stars (F2-12) was inferred to be variable star by Adén et al. (2009a). The other star, (F2-17), was recently classified as a variable star in Hercules by Musella et al. (2012).

The spatial distribution of the members is shown in the right hand panel of Fig.3 by the star symbols. The blue dots give the distribution of RGB (+2 RHB-AGB) stars (with spectra) from Adén et al. (2009a). We confirm previous inferences from photometry that *Hercules has an extended, elongated structure.*

### 3.1 Bound or un-bound?

Are these distant stars bound to Hercules? In Figure 4, we show the velocity relative to the systemic velocity of Hercules as a function of projected distance. We assume isotropic orbits and consider the (1D) escape velocity (i.e.  $V_{\text{esc},1D} = V_{\text{esc},3D}/\sqrt{3}$ ) for Navarro-Frenk-White (NFW; Navarro et al. 1996) halo models. Three different halo masses are shown ( $M_{200} = 10^7, 10^{7.5}, 10^8 M_{\odot}$ ) by the solid, dotted and dashed lines. We show three different halo concentration models given by the black ( $c_{200} = 10$ ), purple ( $c_{200} = 20$ ) and cyan ( $c_{200} = 50$ ) lines.

This figure shows that two of the possible Hercules members at large distances are almost certainly unbound. Even discounting these two possible members, the remaining three distant members favour large halo masses of  $M_{200} \sim 10^8 M_{\odot}$ . Are these models consistent with previous mass estimates of Hercules? Adén et al. (2009b) measure a mass of  $M = 2 \times 10^6 M_{\odot}$  within 300 pc. The massive halo models of  $M_{200} \sim 10^8 M_{\odot}$  are only consistent with this measurement if the concentration is very low,  $c_{200} < 10$ . This is not in agreement with the very high concentrations predicted in cold dark matter simulations (e.g. Bullock et al. 2001). Similarly, halo models of  $M_{200} \sim 10^{7.5} M_{\odot}$  require concentrations of  $c_{200} < 20$  to be consistent with the Adén et al. (2009b) measurement.

It is worth considering how likely it is that these 3 distant Hercules stars are drawn from the same velocity distribution as the central field (field 2) stars. We assume that the velocity distribution for the central field members is a Gaussian with mean  $v_0 \sim 0$  and dispersion  $\sigma_V \sim 9 \text{ km s}^{-1}$ . The likelihood of the three distant member velocities, given this model, is then:

$$L = \prod_{i=1}^3 \frac{1}{\sqrt{2\pi}\sqrt{\sigma^2 + \sigma_i^2}} \exp\left(-\frac{(v_i - v_0)^2}{2(\sigma^2 + \sigma_i^2)}\right) \quad (2)$$

Here,  $\sigma_i$  is the uncertainty in the velocity measurement. We infer the significance of this likelihood by generating control samples of 3 stars drawn randomly from the central field velocity distribution. After  $10^5$  trials, we find that the likelihood of the three distant stars is less than the control samples 74 % of the time. Thus, it is unlikely that these distant stars are drawn from the same velocity distribution as the central field. Note that if the 2 stars with significant velocity differences are included in this test, then the likelihood is less than the control sample likelihood in all trials.

We conclude that if these stars are members of Hercules then it is very unlikely that they are bound. *The presence of unbound members in addition to the elongated structure of Hercules strongly suggests that this dwarf is being tidally disrupted.*

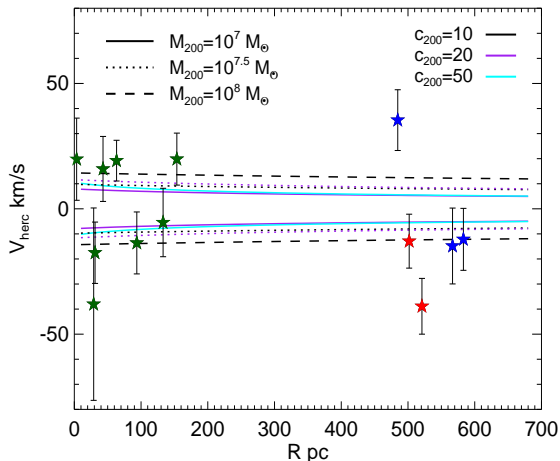


**Figure 4.** Line of sight velocity relative to the systemic velocity of Hercules ( $45 \text{ km s}^{-1}$ ). The filled star symbols are the likely Hercules members. The lines show escape velocity profiles for NFW models assuming isotropic orbits (i.e.  $V_{\text{esc},1D} = V_{\text{esc},3D}/\sqrt{3}$ ). The solid, dotted and dashed lines are for haloes with virial masses of  $M_{200} = 10^7$ ,  $10^{7.5}$  and  $10^8 M_{\odot}$  respectively. The colours indicate concentrations of  $c_{200} = 10$  (black),  $c_{200} = 20$  (purple) and  $c_{200} = 50$  (cyan). Only models with masses within 300 pc consistent with  $M = 1.9^{+1.1}_{-0.8} \times 10^6 M_{\odot}$  (Adén et al. 2009b) are shown.

#### 4 DISCUSSION AND CONCLUSIONS

The spectroscopic confirmation of BHB members at large distances ( $\sim 0.5 \text{ kpc}$ ) in the Hercules dwarf has several implications. First, it gives weight to the detection by Sand et al. (2009) of a narrow, stream-like feature in the Hercules stellar density distribution. Consequently, it resonates with the view in both Adén et al. (2009b) and Martin & Jin (2010) that Hercules may not be a simple bound system in equilibrium. If so, then its mass can not be gauged via the measurement of the overall velocity dispersion and the size (see e.g. Klimentowski et al. 2007; Łokas et al. 2008; Łokas 2009). Additionally, it demonstrates the power of BHBs as robust tracers of the true extent of the low-luminosity stellar systems. Given the properties of the ultrafaint dwarfs, it is unlikely that there would be any significant difference in the epochs and mechanisms of formation of the population of BHBs and of the dominant population of the metal-poor and old main sequence (MS) and RGB stars. Therefore, we argue that in the systems like Hercules, Leo IV, Leo V and Pisces II, the BHBs, which suffer from far less field contamination than MS/RGB tracers, actually reveal the true sizes of the satellites.

Martin & Jin (2010) showed that the available data are consistent with the hypothesis in which Hercules was nothing but a segment of a tidal stream observed near the apocentre. They reasoned, however, that even though there exists a feasible orbit matching the measured properties of the satellite, there is no conclusive evidence in favour of the tidal stream scenario. Still, such a picture has a strong testable prediction: there should be a substantial distance and velocity gradient along the major axis of Hercules. Our data are good enough to argue that the most distant blue stars some 15 arcminutes (or  $> 500 \text{ pc}$ ) away from the dwarf’s centre share the satellites line-of-sight velocity, and, therefore, given their location on the colour magnitude diagram, are probably BHB members of Hercules. Unfortunately, our velocity accuracy is not sufficient to improve on the measurement of the velocity gradient hinted at

by Adén et al. (2009b). Confirmation of, and measurement of, the gradient should be a major goal for future observational studies of Hercules. However, while the presence of a velocity gradient in Hercules would provide compelling evidence that the dwarf is being tidally disrupted, we caution that the lack of a velocity gradient does not necessarily rule out tidal disruption (see e.g. Muñoz et al. 2008).

In summary, we find ample evidence that supports the idea that the Hercules dSph is being tidally stripped. For this ultra-faint dwarf at least, mass estimates must be applied with caution. Wide-field spectroscopic surveys of other ultra-faint dwarf galaxies are needed to determine whether they also have evidence for tidal disruption.

#### ACKNOWLEDGEMENTS

AJD thanks the Science and Technology Facilities Council (STFC) for the award of a studentship, whilst VB acknowledges financial support from the Royal Society. MF acknowledges funding through FONDECYT project No. 1095092 and BASAL. AJD thanks James Clem for providing photometric data of the globular cluster M92. We also thank the anonymous referee, whose comments greatly improved the quality of the Letter.

#### REFERENCES

- Adén D., et al., 2009a, *A&A*, 506, 1147  
 Adén D., Wilkinson M. I., Read J. I., Feltzing S., Koch A., Gilmore G. F., Grebel E. K., Lundström I., 2009b, *ApJ*, 706, L150  
 Belokurov V., et al., 2007, *ApJ*, 654, 897  
 Bullock J. S., Kolatt T. S., Sigad Y., Somerville R. S., Kravtsov A. V., Klypin A. A., Primack J. R., Dekel A., 2001, *MNRAS*, 321, 559  
 Clem J. L., Vanden Berg D. A., Stetson P. B., 2008, *AJ*, 135, 682  
 Coleman M. G., et al., 2007, *ApJ*, 668, L43  
 Deason A. J., Belokurov V., Evans N. W., 2011, *MNRAS*, 416, 2903  
 Klimentowski J., Łokas E. L., Kazantzidis S., Prada F., Mayer L., Mamon G. A., 2007, *MNRAS*, 378, 353  
 Łokas E. L., 2009, *MNRAS*, 394, L102  
 Łokas E. L., Klimentowski J., Kazantzidis S., Mayer L., 2008, *MNRAS*, 390, 625  
 Majewski S. R., Skrutskie M. F., Weinberg M. D., Ostheimer J. C., 2003, *ApJ*, 599, 1082  
 Markwardt C. B., 2009, in D. A. Bohlender, D. Durand, & P. Dowler ed., *Astronomical Data Analysis Software and Systems XVIII* Vol. 411 of ASP Conf. Ser., p. 251  
 Martin N. F., de Jong J. T. A., Rix H.-W., 2008, *ApJ*, 684, 1075  
 Martin N. F., Jin S., 2010, *ApJ*, 721, 1333  
 Muñoz R. R., Geha M., Willman B., 2010, *AJ*, 140, 138  
 Muñoz R. R., Majewski S. R., Johnston K. V., 2008, *ApJ*, 679, 346  
 Muñoz R. R., Padmanabhan N., Geha M., 2012, *ApJ*, 745, 127  
 Musella I., et al., 2012, *ArXiv:1206.4031*  
 Navarro J. F., Frenk C. S., White S. D. M., 1996, *ApJ*, 462, 563  
 Peñarrubia J., Benson A. J., Walker M. G., Gilmore G., McConnachie A. W., Mayer L., 2010, *MNRAS*, 406, 1290  
 Robin A. C., Reylé C., Derrière S., Picaud S., 2003, *A&A*, 409, 523

- Sand D. J., Olszewski E. W., Willman B., Zaritsky D., Seth A.,  
Harris J., Piatek S., Saha A., 2009, *ApJ*, 704, 898  
Schlegel D. J., Finkbeiner D. P., Davis M., 1998, *ApJ*, 500, 525  
Simon J. D., Geha M., 2007, *ApJ*, 670, 313  
Sirko E., et al., 2004, *AJ*, 127, 899  
Zucker D. B., et al., 2006, *ApJ*, 650, L41